



**HAL**  
open science

## Stress and electric field induced phase transitions for ultra high energy conversion in ferroelectrics

Gaspard Taxil, Gael Sebald, Tung Thanh Nguyen, Benjamin Ducharne, Hung Hoang Nguyen, Takahito Ono, Hiroki Kuwano, Mickaël Lallart

### ► To cite this version:

Gaspard Taxil, Gael Sebald, Tung Thanh Nguyen, Benjamin Ducharne, Hung Hoang Nguyen, et al.. Stress and electric field induced phase transitions for ultra high energy conversion in ferroelectrics. Acta Materialia, 2023, 261, pp.119367. 10.1016/j.actamat.2023.119367 . hal-04399401

**HAL Id: hal-04399401**

**<https://hal.science/hal-04399401>**

Submitted on 22 Jan 2024

**HAL** is a multi-disciplinary open access archive for the deposit and dissemination of scientific research documents, whether they are published or not. The documents may come from teaching and research institutions in France or abroad, or from public or private research centers.

L'archive ouverte pluridisciplinaire **HAL**, est destinée au dépôt et à la diffusion de documents scientifiques de niveau recherche, publiés ou non, émanant des établissements d'enseignement et de recherche français ou étrangers, des laboratoires publics ou privés.

# Stress and electric field induced phase transitions for ultra high energy conversion in ferroelectrics

Gaspard Taxil<sup>a,b,c,d,\*</sup>, Gaël Sebald<sup>b,\*</sup>, Tung Thanh Nguyen<sup>b,d</sup>, Benjamin Ducharne<sup>a,b</sup>, Hung Hoang Nguyen<sup>d</sup>, Takahito Ono<sup>c</sup>, Hiroki Kuwano<sup>b,d</sup>, Mickaël Lallart<sup>a</sup>

<sup>a</sup>*Univ. Lyon INSA-Lyon LGEF EA682 F-69621 France*

<sup>b</sup>*ELyTMaX IRL 3757 CNRS Univ. Lyon INSA Lyon Centrale Lyon University Claude Bernard Lyon 1 Tohoku University Sendai Japan*

<sup>c</sup>*Graduate School of Engineering Tohoku University Sendai 9808579 Japan*

<sup>d</sup>*New Industry Creation Hatchery Center (NICHe) Tohoku University 6-6-10 Aramaki-Aoba Aoba-ku Sendai Miyagi 980-8579 Japan*

---

## Abstract

This work focuses on energy harvesting of ferroelectric relaxors PMN-25PT and PZN-8PT single crystals with high uniaxial stress and electric field. Ericsson cycle, which consists of applying and releasing electric field and stress at different steps of the cycle, has been used. A large energy density for PZN-8PT high as 410 mJ/cm<sup>3</sup> was obtained. Different working temperatures were tested by experiment and modeled via Landau-Devonshire theory. Optimal working temperatures were identified for high level energy conversion and were successfully predicted by simulation. It appeared that the optimum

---

\*Corresponding authors

Informations:

Gaspard Taxil: Phone:+81 222176547 (Japan) Adress: Room 502, ELyTMaX Laboratory Material Solutions Center (MaSC), Tohoku University2-1-1 Katahira, Aoba-ku980-8577 Sendai (Japan).

Gaël Sebald: Phone:+81 222176547(Japan) Fax:+81 222176297 Adress: Room 502, ELyT-MaX Laboratory Material Solutions Center (MaSC), Tohoku University2-1-1 Katahira, Aoba-ku980-8577 Sendai (Japan)

*Email addresses:* [gaspard.taxil@insa-lyon.fr](mailto:gaspard.taxil@insa-lyon.fr) (Gaspard Taxil), [gael.sebald@insa-lyon.fr](mailto:gael.sebald@insa-lyon.fr) (Gaël Sebald), [thanhtung1077@gmail.com](mailto:thanhtung1077@gmail.com) (Tung Thanh Nguyen), [benjamin.ducharne@insa-lyon.fr](mailto:benjamin.ducharne@insa-lyon.fr) (Benjamin Ducharne), [nguyen.hoang.hung.a1@tohoku.ac.jp](mailto:nguyen.hoang.hung.a1@tohoku.ac.jp) (Hung Hoang Nguyen), [takahito.ono.d4@tohoku.ac.jp](mailto:takahito.ono.d4@tohoku.ac.jp) (Takahito Ono), [hiroki.kuwano.e5@tohoku.ac.jp](mailto:hiroki.kuwano.e5@tohoku.ac.jp) (Hiroki Kuwano), [mickael.lallart@insa-lyon.fr](mailto:mickael.lallart@insa-lyon.fr) (Mickaël Lallart)

working temperature was different from that optimizing the  $d_{33}$ . Polarization mechanisms induced by these extreme conditions for energy harvesting are explained in the frame of experimental and modeling results. The results obtained at high stress levels tend to indicate that operating along the polarization direction yields the best results, which contradicts conclusions drawn in the case of domain engineered crystals.

*Keywords:* Ferroelectric, phase transition, single crystal, modeling, energy harvesting

---

## 1. Introduction

Energy harvesting is a field in huge growth over the past twenty years. The ability to power devices without battery, which suffer from self-discharge and yield delicate replacement in harsh conditions, has attracted the scientific community. Moreover, the upcoming ecologic transition requires sustainable energy production and energy harvesting can contribute to this challenge. Different sources of energy can be considered for energy harvesting. For instance, wind, solar radiations or vibrations are among the most used. In the field of mechanical energy harvesting, the majority of research works consider resonant devices operating with vibrating mechanical sources [1, 2, 3, 4]. However, there is a lot of random sudden mechanical energy inputs that can be harvested in everyday life (switches, step, tire on road, door opening, etc) [5, 6, 7]. In this context, ferroelectric materials, which are a class of piezoelectric materials, are very promising for such applications due to their remarkable properties. A particularity of these materials is to have a remnant polarization at zero electric field. Another interesting feature is the possibility for these materials to present phase transitions with the variation of temperature, electric field and stress. It is possible to improve energy harvesting by using these phase transitions as the properties of the material are non-linear in the vicinity of these transitions [8, 9]. Ferroelectric relaxors like  $(1 - x)\text{PMN} - x\text{PT}$  and  $(1 - x)\text{PZN} - x\text{PT}$  have been largely investigated [10, 11, 12] due to their outstanding piezoelectric properties, particularly with compositions close to the morphotropic boundary conditions (MPB). In this composition range, these materials easily change their ferroelectric phase via variation of stress and electric field [13, 14]. In this context, this study aims at identifying ideal thermodynamic conditions for

energy harvesting and the contribution of phase transitions to such applicative target in such ferroelectric relaxors. A strong research effort has been made using thermodynamic cycles to increase the output power. The Ericsson cycle, generally called Olsen cycle for pyroelectric energy harvesting, has been investigated due to its high energy conversion abilities [15, 16, 17]. In mechanical energy harvesting, this cycle consists of two isotress processes and two isoelectric processes. This work investigates energy harvesting with Ericsson cycle in PMN-25PT and PZN-8PT with  $\langle 001 \rangle$  orientation under high electric field and uniaxial stress. There is a lack of studies that evaluates their energy conversion abilities with such conditions and the intrinsic mechanisms of polarization involved in such excitations. Thus, this work aims at understanding and identifying ideal polarization mechanisms for energy harvesting in such conditions. In a first step, this study presents a description of the experimental testbench and of the Ericsson cycle. Then a theoretical model based on the Landau-Devonshire theory is proposed to evaluate the energy density with Ericsson cycle. After that, experimental characterization of PMN-25PT and PZN-8PT  $\langle 001 \rangle$  oriented single crystal is made under various conditions of stress and electric field when varying the operating temperature. The experimental results are also compared with simulation and are discussed with the different polarization mechanisms involved in the process. Finally optimal working temperatures for mechanical energy harvesting are identified and explained in the frame of experimental and theoretical results.

## 2. Experimental methods

### 2.1. Materials and experimental testbench

PMN-25PT and PZN-8PT  $\langle 001 \rangle$ -oriented single crystals were respectively purchased from Otsuka corporation, Japan and Microfine Materials technologies, Singapore. Both samples were poled along the  $[001]_c$  direction and have a thickness of 1mm. Samples were cut by a dicing machine DISCO DAD3240. Surface was  $6 \times 6 \text{mm}^2$  for PMN-25PT and of  $2.5 \times 2.5 \text{mm}^2$  for PZN-8PT. A Shimadzu<sup>®</sup> AGS-X series compression test machine was used to apply the desired force on the samples. A Tektronix<sup>®</sup> AFG1022 arbitrary function generator and Trek<sup>®</sup> 10/10B-HS high voltage amplifier were used to apply the electric field. The current was monitored by using a low-noise current amplifier (Stanford research<sup>®</sup>, Sunnyvale, CA, United States of America). Samples for measurements were put in a silicon oil bath to apply

the electric field and regulate the temperature. The temperature was monitored with a Shimadzu<sup>®</sup> TCE-N300A thermostatic chamber. Illustrations of the experimental test-bench and the samples are given in Fig. 1 (a),(b) and (c).

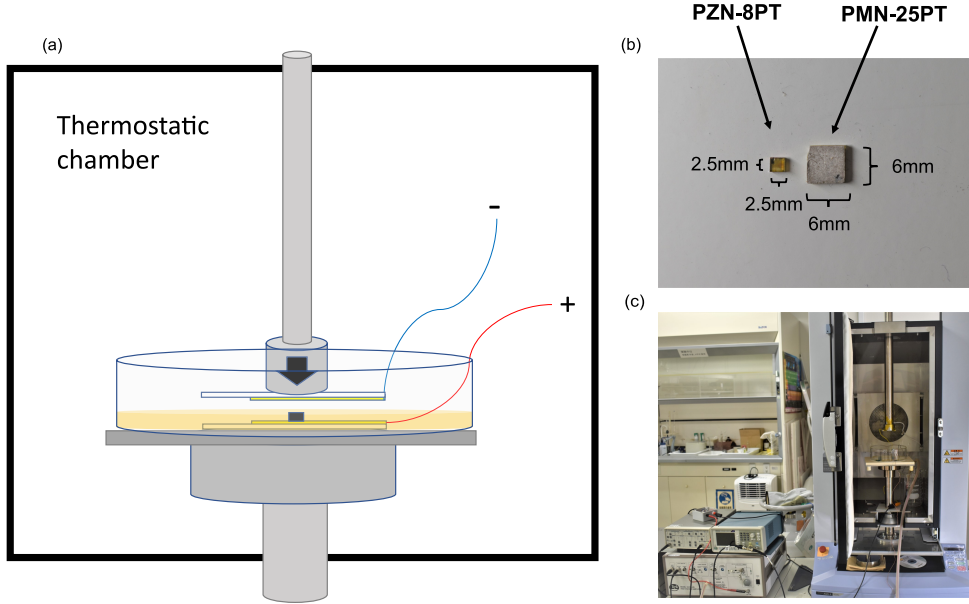


Figure 1: (a) Schematic of the experimental setup; (b) Photograph of PMN-25PT and PZN-8PT single crystals; (c) Photograph of the experimental setup inside the Shimadzu thermostatic chamber.

## 2.2. Ericsson cycle

Mechanical energy harvesting with a single force application requires converting as much as possible of mechanical energy input into electrical one. To achieve this, employing a closed thermodynamic cycle is a good solution due to the high potential of energy conversion [18, 19]. We used Ericsson cycle which consists of starting at zero stress and zero electric field. An electric field is then applied until a final value  $E_f$  is reached (1-2 path in Fig. 2(a)). Then, an uniaxial stress is applied along the electric field direction (2-3 path). Afterwards, the electric field is decreased to zero at high stress level (3-4 path). Finally, the stress is released to close the cycle (4-1 path). Harvested energy is given by the clockwise contour integration of the cycle in the P-E space (Polarization-Electric field) as illustrated in Fig. 2(a). It

can be noted that polarization can be considered as the conjugated variable of the electric field due to the high relative permittivity  $\epsilon_r \gg 1$  in ferroelectrics materials. The directions of the applied stress and electric field were chosen to be along the  $[001]_c$  directions. Illustration of possible polarization mechanism of ferroelectric single crystals during the different steps of an Ericsson cycle is presented in Fig. 2(b). The aim of this study is to determine what are the optimal polarization mechanisms and phase transitions in ferroelectric materials for energy harvesting in these conditions and under high excitation levels.

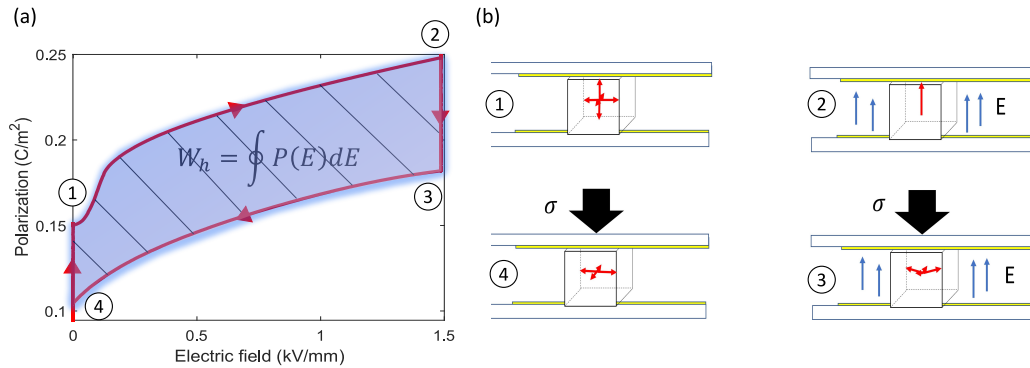


Figure 2: The different possible orientations of the polarization for a ferroelectric crystal. (a) Illustration of the Ericsson cycle; (b) Illustration of polarization mechanisms at the different steps of an Ericsson cycle.

### 3. Phenomenological approach

In order to study phase transitions of ferroelectric materials, the Landau-Devonshire theory has been largely employed during the last decades for ferroelectrics [20, 21, 22]. Few studies proposed to use it for energy harvesting purpose and modeled thermodynamic cycles for pyroelectric energy harvesting [23, 24]. However, none of them proposed to use such an approach for mechanical energy harvesting and make profit of its predictive abilities. To better understand and confirm the experimental results, the Landau phenomenological theory was employed. The free energy is developed as a function of an order parameter which is the polarization for ferroelectrics. By adopting the Einstein summation convention, the classical free energy intro-

duced by Devonshire [25] is expressed as:

$$F_{lgd} = \alpha_{ij}P_iP_j + \alpha_{ijkl}P_iP_jP_kP_l + \alpha_{ijklmn}P_iP_jP_kP_lP_mP_n + \alpha_{ijklmnop}P_iP_jP_kP_lP_mP_nP_oP_p + \dots \quad (1)$$

where  $P_i$  are components of the spontaneous polarization;  $\alpha_{ij}$ ,  $\alpha_{ijkl}$ ,  $\alpha_{ijklmn}$  and  $\alpha_{ijklmnop}$  are tensors representing the different orders of the dielectric stiffness. One significant advantage of this approach is the possibility to take into account the temperature, the electric field and the stress applied to the ferroelectric material. The free enthalpy correspond to the appropriate thermodynamic potential to describe these kinds of systems and is given in tensorial notation by:

$$\Delta G = F_{lgd} - E_iP_i - \frac{1}{2}s_{ijkl}\sigma_{ij}\sigma_{kl} - Q_{ijkl}\sigma_{ij}P_kP_l \quad (2)$$

where  $E_i$  are the electric field components,  $\sigma_{ij}$  is the stress tensor and  $s_{ijkl}$  and  $Q_{ijkl}$  are respectively the compliance and electrostrictive tensors. This free energy must be invariant by symmetry of a parent phase [26, 27] and with respect to the  $m\bar{3}m$  symmetry. By adopting the Voigt notation its expression yields:

$$\begin{aligned} \Delta G = & \alpha_1(P_1^2 + P_2^2 + P_3^2) + \alpha_{11}(P_1^4 + P_2^4 + P_3^4) \\ & + \alpha_{12}(P_1^2P_2^2 + P_1P_3^2 + P_2^2P_3^2) + \alpha_{123}P_1^2P_2^2P_3^2 \\ & + \alpha_{111}(P_1^6 + P_2^6 + P_3^6) + \alpha_{112}\left[P_1^2(P_2^4 + P_3^4) \right. \\ & \left. + P_2^2(P_1^4 + P_3^4) + P_3^2(P_1^4 + P_2^4)\right] + \alpha_{1111}(P_1^8 + P_2^8 \\ & + P_3^8) + \alpha_{1122}(P_1^4P_2^4 + P_1^4P_3^4 + P_2^4P_3^4) \\ & + \alpha_{1112}\left[P_1^6(P_2^2 + P_3^2) + P_2^6(P_1^2 + P_3^2) \right. \\ & \left. + P_3^6(P_1^2 + P_2^2)\right] + \alpha_{1123}(P_1^4P_2^2P_3^2 + P_1^2P_2^4P_3^2 \\ & + P_1^2P_2^2P_3^4) - \frac{1}{2}s_{11}(\sigma_1^2 + \sigma_2^2 + \sigma_3^2) \\ & - s_{12}(\sigma_1\sigma_2 + \sigma_1\sigma_3 + \sigma_2\sigma_3) - \frac{1}{2}s_{44}(\sigma_4^2 + \sigma_5^2 + \sigma_6^2) \\ & - Q_{11}(\sigma_1P_1^2 + \sigma_2P_2^2 + \sigma_3P_3^2) - Q_{12}\left[\sigma_1(P_2^2 + P_3^2) \right. \\ & \left. + \sigma_2(P_1^2 + P_3^2) + \sigma_3(P_1^2 + P_2^2)\right] - Q_{44}(\sigma_4P_2P_3 + \sigma_5P_1P_3 \\ & + \sigma_6P_1P_2) - E_1P_1 - E_2P_2 - E_3P_3 \end{aligned} \quad (3)$$

As we applied the electric field and the stress along the  $[001]_c$  direction ( $E_1 = E_2 = 0$  and  $\sigma_1 = \sigma_2 = 0$  and  $\sigma_4 = \sigma_5 = \sigma_6 = 0$ ), the expression is reduced

to:

$$\begin{aligned}
\Delta G = & \alpha_1(P_1^2 + P_2^2 + P_3^2) + \alpha_{11}(P_1^4 + P_2^4 + P_3^4) \\
& + \alpha_{12}(P_1^2P_2^2 + P_1P_3^2 + P_2^2P_3^2) + \alpha_{123}P_1^2P_2^2P_3^2 \\
& + \alpha_{111}(P_1^6 + P_2^6 + P_3^6) + \alpha_{112} \left[ P_1^2(P_2^4 + P_3^4) \right. \\
& + P_2^2(P_1^4 + P_3^4) + P_3^2(P_1^4 + P_2^4) \left. \right] + \alpha_{1111}(P_1^8 + P_2^8 \\
& + P_3^8) + \alpha_{1122}(P_1^4P_2^4 + P_1^4P_3^4 + P_2^4P_3^4) \\
& + \alpha_{1112} \left[ P_1^6(P_2^2 + P_3^2) + P_2^6(P_1^2 + P_3^2) \right. \\
& + P_3^6(P_1^2 + P_2^2) \left. \right] + \alpha_{1123}(P_1^4P_2^2P_3^2 + P_1^2P_2^4P_3^2 \\
& + P_1^2P_2^2P_3^4) - \frac{1}{2}s_{11}\sigma_3^2 - Q_{11}\sigma_3P_3^2 - Q_{12}\sigma_3(P_1^2 + P_2^2) - E_3P_3
\end{aligned} \tag{4}$$

By minimizing the free enthalpy with respect to polarization, it is thus possible to obtain for each thermodynamic state its associated polarization. Depending on electric field and stress and their directions of application, different phase configurations are possible and are highlighted in Table 1.

In the experiments, the polarization is obtained through the variation of the current flowing to the samples. The crystals are  $\langle 001 \rangle$  oriented, thus, the measured polarization is a projection along the z axis ( $P_3$ ). In the modeling, only the tetragonal (T), orthorhombic (O) and rhombohedral (R) states were considered and are illustrated in Fig.3 (a). The monoclinic phases are not considered here as PZN-8PT was limited to the sixth order expansion [28]. When the electric field and stress are applied at the same

State	Polarization components	Number of configuration	Symmetry	Domain structure
Cubic $\langle 001 \rangle$	(0, 0, 0)	1	$m\bar{3}m$	
Tetragonal $\langle 001 \rangle$	(0, 0, $P$ )	6	4mm	1T
Orthorhombic $\langle 001 \rangle$	$(\frac{P}{\sqrt{2}}, \frac{P}{\sqrt{2}}, 0)$	12	mm2	4O
Rhombohedral $\langle 001 \rangle$	$(\frac{P}{\sqrt{3}}, \frac{P}{\sqrt{3}}, \frac{P}{\sqrt{3}})$	8	3m1	4R

Table 1: Properties of the different ferroelectric phases

time, it is difficult to predict which state will adopt the crystal as the electric field tends to favor a direction along its direction of application as shown in Fig. 3 (b), while uniaxial stress tends to favor perpendicular states to its direction of application as represented in Fig. 3 (c). Thus, the modeling is used here for its ability to predict the state of the crystal for each step of the Ericsson cycle. The phenomenological coefficients for PMN-25 PT were taken from [29] and the coefficients for PZN-8PT were derived from a mixing law [30] of the coefficients of [31]. It can be noted that some approximations are made in the simulations. We considered a single domain crystal which is not the case in a real experiment. However, under a sufficient electric field this approximation is quite accurate [32]. Hysteresis of the material is not considered and linear response with stress of the polarization is largely underestimated. Indeed, simulations predicts a piezoelectric coefficient of  $d_{33} \approx 10^2 pC/N$  while  $d_{33} \approx 10^3 pC/N$  in PMN-25PT and PZN-8PT [33, 34]. Nevertheless, the modeling is more dedicated to qualitatively predict which ferroelectric phase is optimal in given working conditions.

#### 4. Results and discussion

PMN-25PT and PZN-8PT were first experimentally investigated at different stress levels (0 to 100 MPa). Bipolar loops (electric field from -1500kV/m to 1500kV/m at a frequency of 3Hz) for different values of stress were measured at room temperature and are given in Fig. 4(a) and (b). It can be noted that we limited the electric field value to avoid dielectric breakdown, even if larger electric field has been successfully applied to a single crystal in previous works [35]. However, we set the limit of 1500 kV/m for safety reasons and for achievable values for possible future engineering purpose. The associated remnant and saturation polarization depending on uniaxial stress are depicted in Fig. 4(c) and (d). For both PMN-25PT and PZN-8PT, the coercive field ( $E_c$ ) decreases with applied stress. This phenomena is well known and was already observed [36, 37]. The polarization variation of both materials with applied stress was found to exhibit a different behavior. Indeed, PMN-25PT presents a quasi full linear response of remnant and saturation polarizations with applied stress. This indicates a quasi-constant  $d_{33}$  response with applied stress. However for PZN-8PT, the response of polarization under and without electric field is highly non-linear with an uniaxial stress from 0 to 40MPa and quasi linear from 40 to 100MPa. The high non-linearity in the 0-40 MPa range implied that the  $d_{33}$  is non-constant

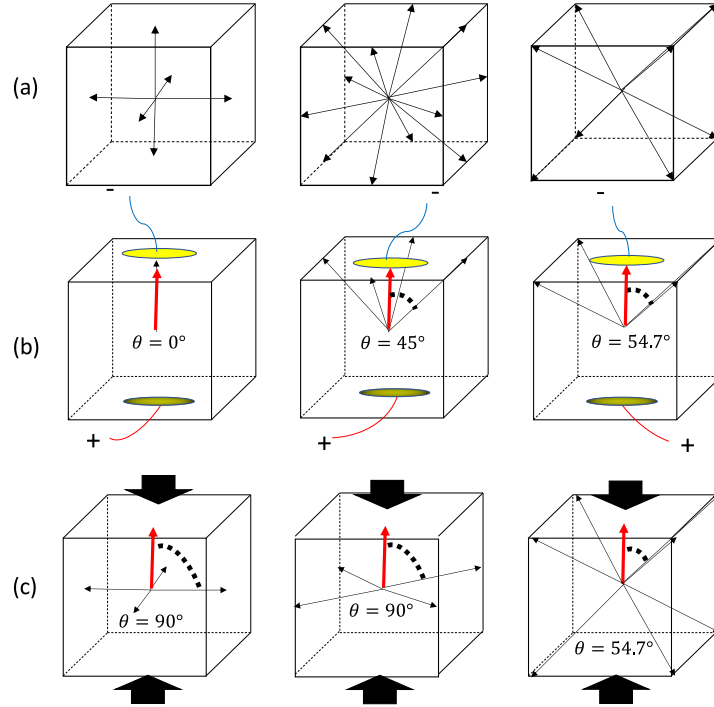


Figure 3: The different possible orientations of polarization for tetragonal, orthorhombic and rhombohedral (left to right) single crystal. (a) Possible configurations without applied electric field and stress; (b) Possible configurations when an electric field is applied; (c) Possible configurations when an uniaxial stress is applied.

with stress. The use of a  $d_{33}$  here is then complex as the large polarization variations are due to in-plane switching of polarization.

Energy harvesting abilities were evaluated by the descending curves of bipolar loops at 0 and 100 MPa. It can be noted that small differences exist between the evaluation of the harvested energy with the descending curves of bipolar loops and real Ericsson cycles. In the latter, hysteresis losses occur due to repolarization of the sample in the 1-2 process (electric field application). Despite these differences, we opted for the evaluation of the harvested energy via bipolar loops due to experimental setup limitation and theoretical considerations. Indeed, current losses occur during Ericsson cycle due to the time of application of the stress. Moreover, the modeled Ericsson cycle with Landau-Devonshire corresponds to these descending curves of bipolar loops. The "Ericsson cycle" term will now refers to the cycle enclosed in the

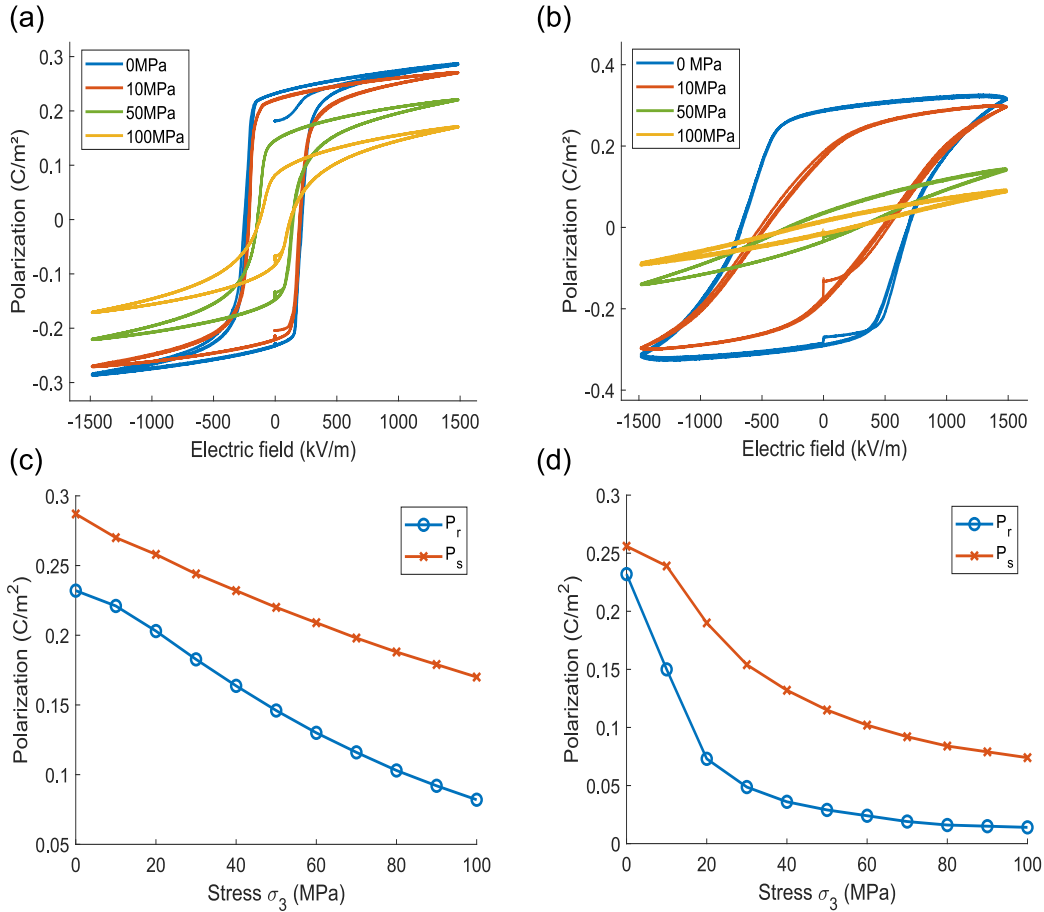


Figure 4: (a) Double hysteresis loops of PMN-25PT under different uniaxial stress; (b) Double hysteresis loops of PZN-8PT under different uniaxial stress; (c) Remnant and saturation polarization of PMN-25PT under different uniaxial stress; (d) Remnant and saturation polarization of PZN-8PT under different uniaxial stress.

descending curves of bipolar loops.

Associated hysteresis curves at 0 and 100MPa are presented for both PMN-25PT and PZN-8PT at different temperatures with their associated Ericsson cycle in Fig. 5. For PMN-25PT (Fig. 5 (a),(c),(e) and (g)), the coercive field decreased with temperature which is generally linked with an increase of piezoelectric properties [38]. It is well understood as the energy barrier decreased with temperature. Thus, lower electric field will permit

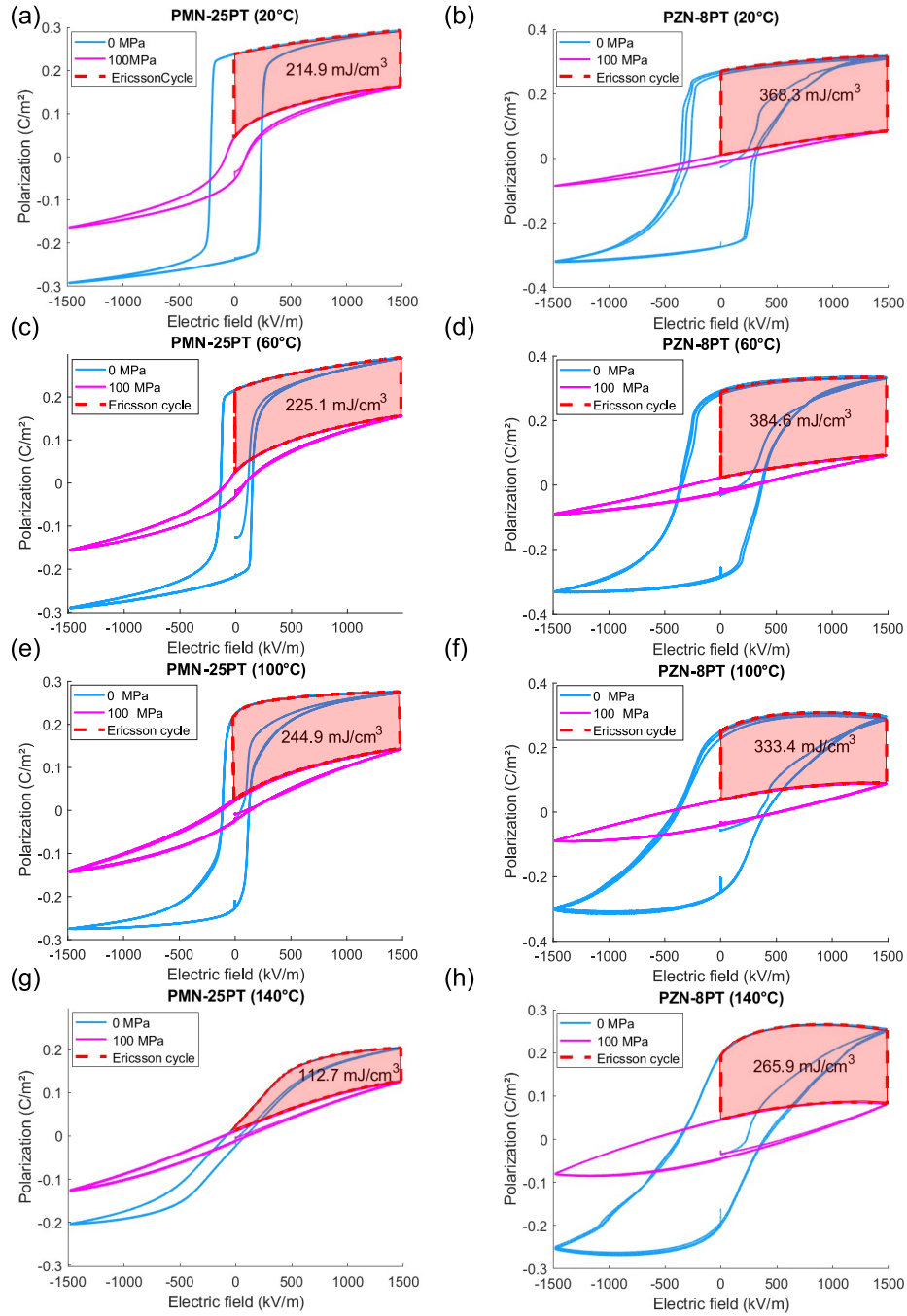


Figure 5: Bipolar loops of PMN-25PT and PZN-8PT with their associated Ericsson cycle at different temperature. (a) PMN-25PT at 20°C; (b) PZN-8PT at 20°C; (c) PMN-25PT at 60°C; (d) PZN-8PT at 60°C; (e) PMN-25PT at 100°C; (f) PZN-8PT at 100°C ; (g) PMN-25PT at 140°C; (h) PZN-8PT at 140°C.

the domains to realign. However, PZN-8PT has a different behavior as  $E_c$  remains constant from 20 to 140°C as shown in Fig. 5 (a),(d),(f) and (h). It is also possible to observe that dielectric losses increased with temperature.

In order to better understand materials response and identify the best polarization mechanisms for energy harvesting, experimental results of polarization components  $P_3$  depending on the applied electric field  $E_3$  and uniaxial stress  $\sigma_3$  of  $\langle 001 \rangle$  PMN-25PT single crystal at different temperature are presented in Fig. 6 (a), (c) and (e). Their associated simulated phase diagrams with Landau-Devonshire theory are depicted in Fig. 6 (b), (d) and (f). At room temperature, the experimental results (Fig. 6 (a)) gave a flat surface of polarization corresponding to a full linear response of the material with stress and electric field. PMN-25PT at this temperature is rhombohedral (R), which was also predicted by the theoretical model. However, the simulation predicts an in-plane switching of polarization perpendicular to  $E_3$  denoted by  $T_{\perp}$  under high stress and low electric field but it was not observed experimentally. At 50°C, the material is still rhombohedral. Modeling indicates a phase transition from rhombohedral to an in-plane phase (tetragonal or orthorhombic). It can be observed in Fig. 6 (c) such a transformation with a non-linear response of polarization in the region delimited from 0 to 500kV/m and from 50 to 100MPa (low electric field, high stress), as it was already reported in the literature for  $(1-x)\text{PMN} - x\text{PT}$  [37, 39, 40]. The spontaneous polarization from 20°C to 50°C drops down in both modeling and characterization as the entropy rises and induces disorder. However, from 50°C to 80°C the spontaneous polarization was both measured and calculated to increase. This indicated the appearance of a tetragonal phase instead of the rhombohedral one. Indeed, we measured and calculated the z projection of polarization in the cubic basis as the crystal is  $\langle 001 \rangle$  oriented. Thus, the polarization projection is higher for the tetragonal phase as its spontaneous polarization is along the  $[001]_c$  direction ( $[111]_c$  for rhombohedral). The measured polarization largely increases from 0 to 500kV/m compared to the 500 to 1500kV/m range in Fig. 6 (e). This points out a rhombohedral-tetragonal transition with the electric field which was already observed and predicted [40, 41, 42]. This R-T transition is also confirmed by the phenomenological approach to appear under the application of the electric field at low stress and is denoted by  $T_{//}$  (polarization aligns with electric field) in Fig. 6 (f). Under high stress and low electric field, experiment and modeling still present 90° switching of polarization. The region

where the polarization is in-plane seems to grow from 50°C to 80°C in the experiment. This easing with temperature for the polarization to adopt a phase perpendicular to the applied electric field direction is also assessed by calculations. PMN-25PT changes with the increasing temperature from a pure linear regime of polarization with the applied stress and electric field to a more complex behavior with appearance of the T// phase and in-plane phases (T $\perp$ ).

PZN-8PT single crystal has been also investigated at different temperature under high uniaxial stress  $\sigma_3$  and electric field  $E_3$  (Fig. 7). It shows different response for the polarization projection  $P_3$  compared to PMN-25PT. Indeed, in Fig. 7(a) at 20°C, a strong non-linear response of the polarization occurred under low stress from 0 to 50MPa and also under high applied electric field. From 50 to 100MPa, polarization varied linearly with the electric field and stress. This linear behavior is explained by a transverse dielectric response of the material in the  $[001]_c$  direction as the spontaneous polarization is switched out in a 90° ferroelectric state. Theoretical calculation in Fig. 7 predicted a R-T transition and agreed well with the perpendicular orientation of the spontaneous polarization under high stress. There is no significant difference of response for PZN-8PT with temperature. Indeed, experimental curves are quite similar between 20°C and 50°C (Fig. 7 (a) and (c)). Nevertheless, literature [43] and experience suggest that the material is in tetragonal state at 50°C as the remnant polarization at 0MPa is slightly higher compared to the one at 20°C which is typical of R-T transitions in  $\langle 001 \rangle$  oriented crystal. The crystal remained in rhombohedral state in the modeling as the R-T transition is predicted to occur at 60°C with the Landau coefficients we have used. Like for PMN-25T, simulation gives an easing of in-plane domain switching with temperature increase (Fig. 7 (d)). The characterization results at 80°C confirmed that the PZN-8PT response with stress and electric field does not vary much with the temperature. Indeed, experimental curves of PZN-8PT at different temperatures are almost identical (Fig. 7 (a), (c) and (e)). Spontaneous polarization at 80°C drops slightly compared to 50°C as disorder increases. Modeling suggests that the material is in tetragonal state and switches out to a perpendicular tetragonal state with low applied stress whatever the applied electric field.

Polarization dependence with uniaxial stress, electric field and temperature was first investigated. Energy harvesting abilities strongly depend of it.

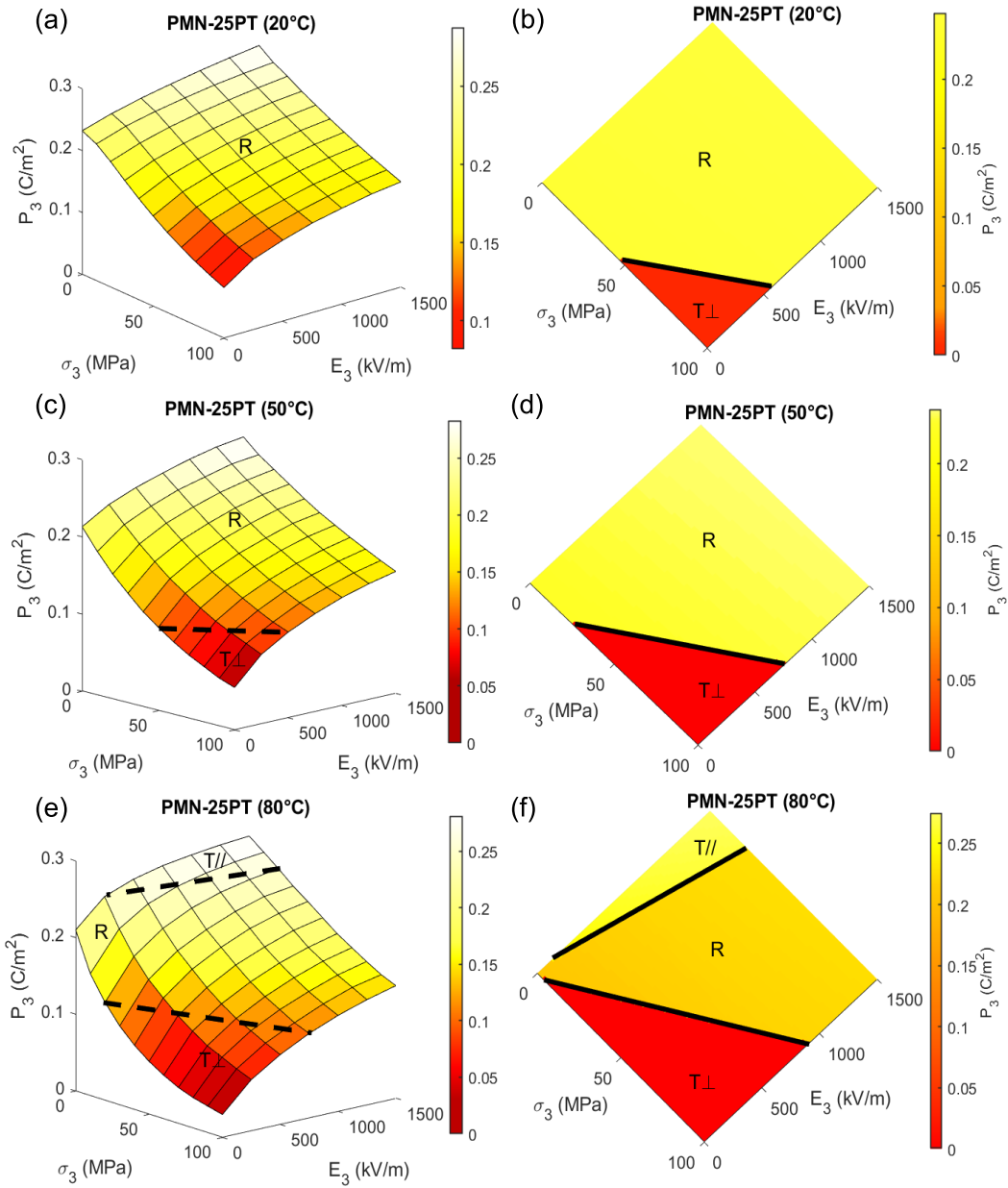


Figure 6: Plot of the component of polarization  $P_3$  depending of uniaxial stress  $\sigma_3$  and electric field  $E_3$  for PMN-25PT. (a) Experiment at 20°C; (b) Modeling at 20°C; (c) Experiment at 50°C; (d) Modeling at 50°C; (e) Experiment at 80°C; (f) Modeling at 80°C.

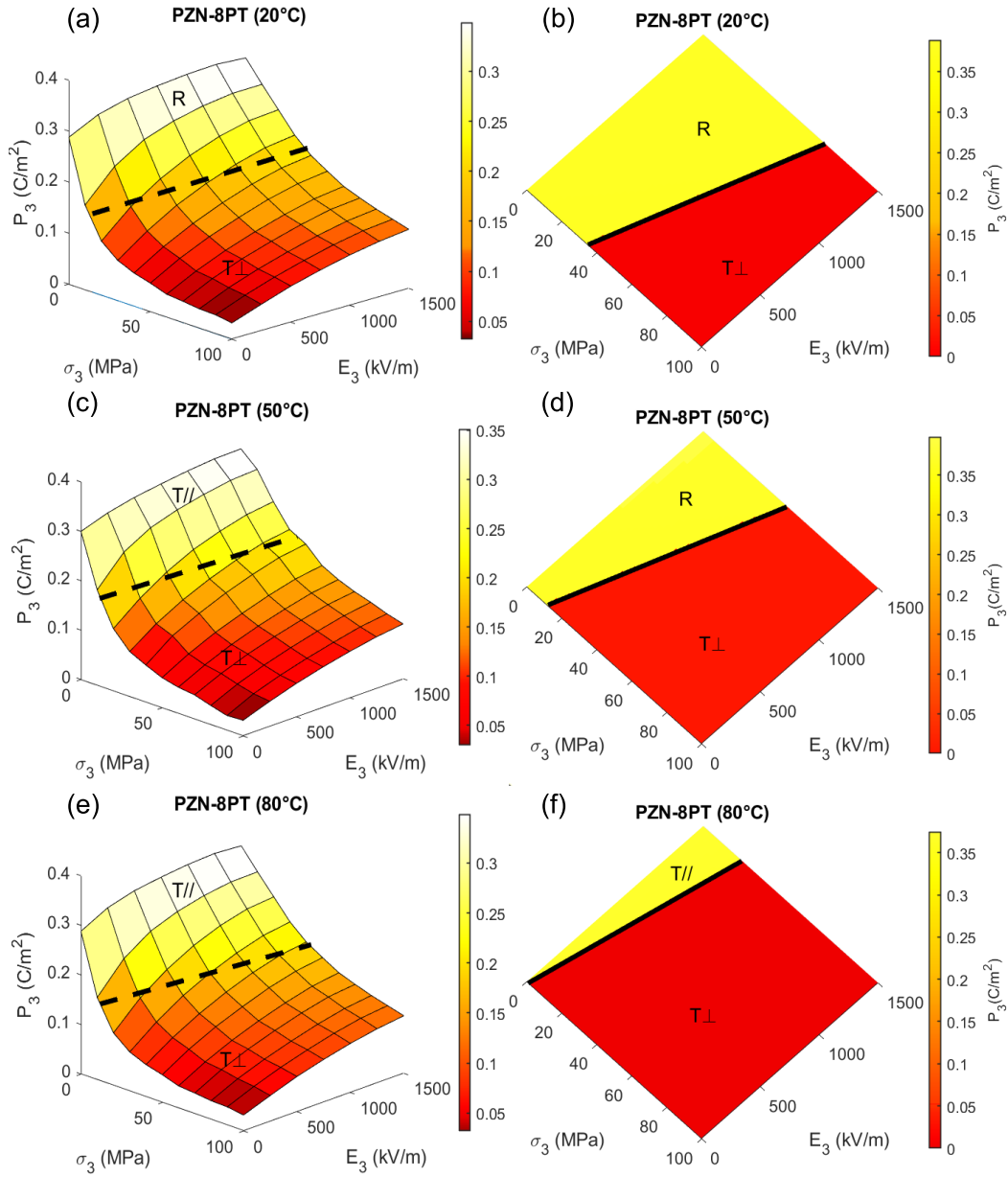


Figure 7: Plot of the component of polarization  $P_3$  depending of uniaxial stress  $\sigma_3$  and electric field  $E_3$  for PZN-8PT. (a) Experiment at 20°C; (b) Modeling at 20°C; (c) Experiment at 50°C; (d) Modeling at 50°C; (e) Experiment at 80°C; (f) Modeling at 80°C.

The next step was to evaluate energy conversion of PMN-25PT and PZN-8PT single crystals with Ericsson cycles. Different operating temperatures were tested while keeping identical Ericsson cycle conditions (stress from 0 to 100MPa and electric field from 0 to 1500kV/m). Experimental and simulated results via phenomenological approach is presented in Fig. 8.

PMN-25PT (Fig. 8 (a) and (b)) energy density has an increasing trend from room temperature to 80°C which corresponds to the rhombohedral-tetragonal (R-T) transition temperature. Energy density varies in this range of temperature from 210mJ/cm<sup>3</sup> to 260mJ/cm<sup>3</sup>. This raise of energy density for PMN-25PT is explained by the easing of 90° domain switching with stress when temperature increases as observed in Fig. 6. These in-planes switching of polarization induce larger polarization variation with stress increasing the cycle area (energy harvested). The modeling predicted a larger increase of harvested energy at 60°C due to the appearance of the tetragonal phase when sufficient electric field is applied. It is barely visible on the experimental curve even if it possible to observe a slightly larger rise of energy around 70°C. A maximum of energy density was observed at 80°C for both experiment and modeling associated to a transition towards complete tetragonal phase of the material. The remnant polarization is maximum for <001> oriented crystals in tetragonal phase. Thus, the possible polarization variation is maximized when in-plane switching occurs and so is the energy density at the R-T transition. Afterwards, energy density remained almost constant experimentally from 80°C to 100°C and from 80°C to 115°C for modeling. This behavior originates from compensation of two phenomena. First, spontaneous polarization drops off due to entropy increase and induces lesser polarization variations, thus the harvested energy decreases. However, in-plane states of polarization are still facilitated under stress when temperature increases. This leads to a near constant evolution of energy density in this temperature range. Finally, energy density decreased largely from 110° to 140°C. It decreased from 250mJ/cm<sup>3</sup> to 110mJ/cm<sup>3</sup>. This behavior is explained by the drop off of polarization when crossing the ferroelectric-paraelectric transition of PMN-25PT. Indeed, a Curie temperature of 110°C was measured and has already been reported [44, 45]. The modeling predicted the same trend for PMN-25PT but with a slight shift towards higher temperatures.

Regarding PZN-8PT (Fig. 8 (c) and (d)), it can be noted that its en-

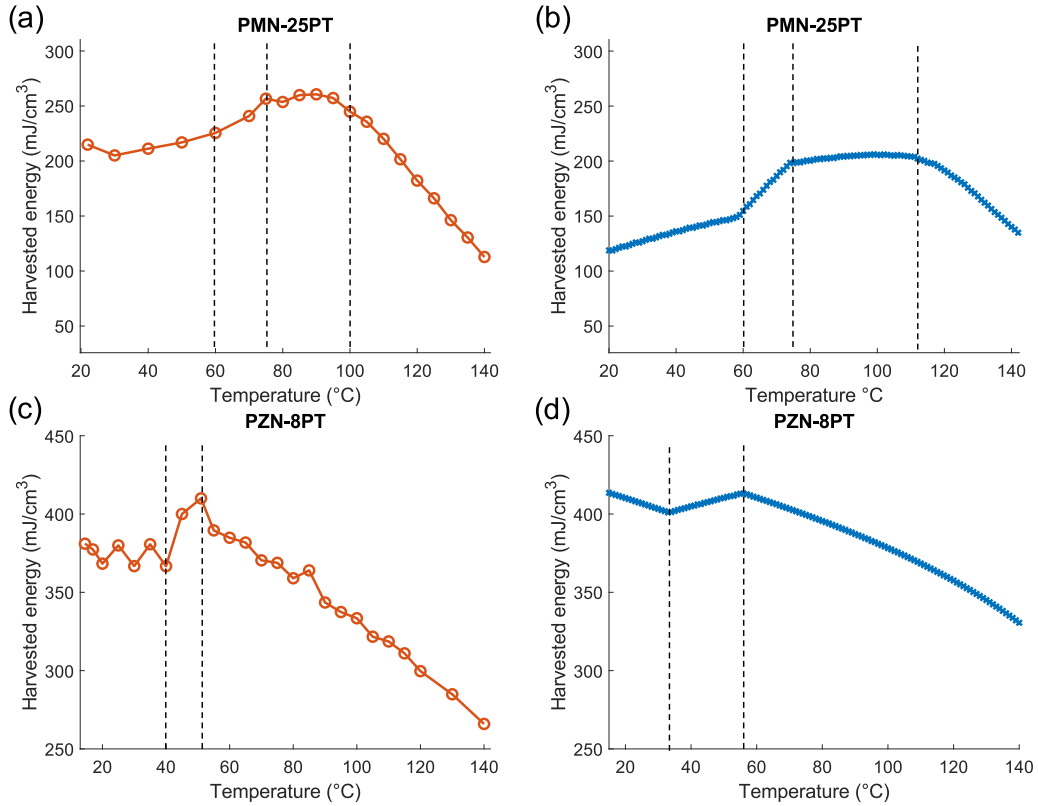


Figure 8: Plot of the energy density depending of the temperature of work of the cycle. (a) Experiment for PMN-25PT; (b) Modeling for PMN-25PT; (c) Experiment for PZN-8PT; (d) Modeling for PZN-8PT.

ergy density is approximately twice of that of PMN-25PT. Nevertheless, it presents a different trend with working temperature. Experimental results indicate a constant energy harvested of approximately  $375\text{mJ}/\text{cm}^3$  from  $20^\circ\text{C}$  to  $40^\circ\text{C}$ . Afterwards, energy density increases from  $40^\circ\text{C}$  until  $55^\circ\text{C}$  where it reaches a maximum of  $410\text{mJ}/\text{cm}^3$ . This rising trend appeared also in simulations and as for PMN-25PT, it originated from the R-T transition under electric field which increases the spontaneous polarization. Concerning the simulations for the  $20\text{-}40^\circ\text{C}$  temperature range, a decrease of harvested energy can be observed. This comes from the lowering of the polarization of the rhombohedral phase as operating temperature increases. However, it was not observed experimentally where the energy remained nearly constant, although the reasons for this are still unclear. Like PMN-25PT, en-

ergy conversion is maximum at the R-T transition, for similar reasons. It is interesting to note that the maximum of energy density of  $410\text{mJ}/\text{cm}^3$  is especially high. To the best knowledge of the authors, no work reported so far such a high energy conversion with these levels of electric field and uniaxial stress. Nevertheless, we can mention the work of Patel et al. [19, 46], who obtained higher energy conversion with Ericsson cycle but with much higher stress ( $\approx 400\text{MPa}$ ) and electric field ( $\approx 2000$  to  $6000\text{ kV}/\text{m}$ ). After  $55^\circ\text{C}$ , both model and experiments gave a decreasing energy until  $140^\circ\text{C}$ . This is again explained by the decrease of spontaneous polarization as disorder and entropy increase with temperature. It can be noticed that the rate of decay of the experimental curve is larger than the theoretical one. It could be explained by the dielectric losses that are more pronounced at higher temperature for PZN-8PT as it was observed in Fig. 5 (a),(d),(f) and (h).

## 5. Conclusion

In this study we characterized and modeled PMN-25PT and PZN-8PT  $\langle 001 \rangle$ -oriented single crystal with Ericsson cycle in the framework of mechanical energy harvesting. An especially high energy density of  $410\text{mJ}/\text{cm}^3$  was obtained. An innovative approach to model thermodynamic cycles for mechanical energy harvesting was proposed based on the Landau-Devonshire theory. The characterization of these crystals under high uniaxial stress and electric field was also reported. Ideal working temperature for electromechanical Ericsson cycle was identified for both crystals. The different results indicated that optimal operation is achieved at the temperature where the crystal became fully tetragonal. This result could be generalized for all  $\langle 001 \rangle$  oriented ferroelectric crystals at sufficient stress where in-plane switching is possible. Indeed, larger polarization variation with high uniaxial stress is possible along the spontaneous polarization direction. An interesting feature of these ferroelectric relaxors is the possibility to tailor the FE-FE temperature transition by adjusting their mixing proportions for future engineering devices. Future studies could investigate  $\langle 011 \rangle$  and  $\langle 111 \rangle$  oriented crystal in order to see if optimal ferroelectric phases are respectively orthorhombic and rhombohedral at high stress levels. Rhombohedral single crystals are known to exhibit the highest  $d_{33}$  when polarized along  $[001]_c$  direction, which is associated with the concept of domain engineering. For high level energy harvesting, our results suggest on the contrary that the direction of the spontaneous polarization would be preferable. However, dif-

ferent aspects were not considered in this study. It is known that PMN-25PT and PZN-8PT polar nano-regions appear at high temperature and give other contributions to the polarization [47, 48, 49]. We also did not take into account the dielectric losses of the materials. In the modeling, only a single domain was considered. Moreover the linear piezoelectric coefficients predicted by the Landau-Devonshire theory is an order of magnitude lower than the measured ones for highly piezoelectric perovskites. Yet, the model proved to be accurate in terms of energy density conversion predictions. Moreover, predictions of in-plane switching under electric field and stress were in good agreements with experiments. To conclude, this work could give guidelines for future energy harvesting studies, materials and devices working at high stress levels.

## **Acknowledgements**

This work was performed under the framework of the ANR-FIESTA project, funded by the French Agence Nationale pour la Recherche, grant ANR-20-CE05-0026, and under the framework of the International Research Network ELyT Global (project FIESTA).

## **AUTHOR DECLARATIONS**

### **Conflict of Interest**

The authors have no conflicts to disclose.

### **Data Availability Statement**

The data that support the findings of this study are available from the corresponding author upon reasonable request.

## **References**

- [1] S. P. Beeby, M. J. Tudor, N. M. White, Energy harvesting vibration sources for microsystems applications, *Measurement Science and Technology* 17 (2006) R175.
- [2] S. Mun, H.-U. Ko, L. Zhai, S.-K. Min, H.-C. Kim, J. Kim, Enhanced electromechanical behavior of cellulose film by zinc oxide nanocoating and its vibration energy harvesting, *Acta Materialia* 114 (2016) 1–6.

- [3] G. Clementi, G. Lombardi, S. Margueron, M. A. Suarez, E. Lebrasseur, S. Ballandras, J. Imbaud, F. Lardet-Vieudrin, L. Gauthier-Manuel, B. Dulmet, M. Lallart, A. Bartasyte, Linbo<sub>3</sub> films – a low-cost alternative lead-free piezoelectric material for vibrational energy harvesters, *Mechanical Systems and Signal Processing* 149 (2021) 107171.
- [4] X. Yan, M. Zheng, X. Gao, L. Li, J. Rödel, M. Zhu, Y. Hou, Ultra-high energy harvesting performance in lead-free piezocomposites with intragranular structure, *Acta Materialia* 222 (2022) 117450.
- [5] S. Ahmad, M. Abdul Mujeebu, M. A. Farooqi, Energy harvesting from pavements and roadways: A comprehensive review of technologies, materials, and challenges, *International Journal of Energy Research* 43 (2019) 1974–2015.
- [6] N. Sharpes, D. Vučković, S. Priya, Floor tile energy harvester for self-powered wireless occupancy sensing, *Energy Harvesting and Systems* 3 (2016) 43–60.
- [7] X. Xu, D. Cao, H. Yang, M. He, Application of piezoelectric transducer in energy harvesting in pavement, *International Journal of Pavement Research and Technology* 11 (2018) 388–395.
- [8] A. Khodayari, S. Pruvost, G. Sebald, D. Guyomar, S. Mohammadi, Non-linear pyroelectric energy harvesting from relaxor single crystals, *IEEE Transactions on Ultrasonics, Ferroelectrics, and Frequency Control* 56 (2009) 693–699.
- [9] D. Guyomar, S. Pruvost, G. Sebald, Energy harvesting based on fe-fe transition in ferroelectric single crystals, *IEEE Transactions on Ultrasonics, Ferroelectrics, and Frequency Control* 55 (2008) 279–285.
- [10] Z. Yang, J. Zu, Comparison of pzn-pt, pmn-pt single crystals and pzt ceramic for vibration energy harvesting, *Energy Conversion and Management* 122 (2016) 321–329.
- [11] S.-E. Park, T. Shrout, Characteristics of relaxor-based piezoelectric single crystals for ultrasonic transducers, *IEEE Transactions on Ultrasonics, Ferroelectrics, and Frequency Control* 44 (1997) 1140–1147.

- [12] K. Rajan, M. Shanthi, W. Chang, J. Jin, L. Lim, Dielectric and piezoelectric properties of [001] and [011]-poled relaxor ferroelectric pzn-pt and pmn-pt single crystals, *Sensors and Actuators A: Physical* 133 (2007) 110–116.
- [13] M. Davis, Picturing the elephant: Giant piezoelectric activity and the monoclinic phases of relaxor-ferroelectric single crystals, *Journal of Electroceramics* 19 (2007) 25–47.
- [14] H. H. Wu, R. E. Cohen, Electric-field-induced phase transition and electrocaloric effect in pmn-pt, *Phys. Rev. B* 96 (2017) 054116.
- [15] R. B. Olsen, D. A. Bruno, J. M. Briscoe, Pyroelectric conversion cycles, *Journal of Applied Physics* 58 (1985) 4709–4716.
- [16] P. Lheritier, A. Torello Massana, T. Usui, Y. Nouchokgwe, A. Aravindhnan, J. Li, U. Prah, V. Kovacova, O. Bouton, S. Hirose, E. Defay, Large harvested energy with non-linear pyroelectric modules, *Nature* 609 (2022) 1–4.
- [17] I. M. McKinley, R. Kandilian, L. Pilon, Waste heat energy harvesting using the olsen cycle on  $0.945\text{Pb}(\text{Zn}_{1/3}\text{Nb}_{2/3})\text{O}_3 - 0.055\text{PbTiO}_3$  single crystals, *Smart Materials and Structures* 21 (2012) 035015.
- [18] N. Tung, G. Taxil, H. Nguyen, B. Ducharne, M. Lallart, E. Lefeuvre, H. Kuwano, G. Sebald, Ultimate electromechanical energy conversion performance and energy storage capacity of ferroelectric materials under high excitation levels, *Applied Energy* 326 (2022) 119984.
- [19] S. Patel, A. Chauhan, R. Vaish, A technique for giant mechanical energy harvesting using ferroelectric/antiferroelectric materials, *Journal of Applied Physics* 115 (2014) 084908.
- [20] J. J. Wang, P. P. Wu, X. Q. Ma, L. Q. Chen, Temperature-pressure phase diagram and ferroelectric properties of batio<sub>3</sub> single crystal based on a modified landau potential, *Journal of Applied Physics* 108 (2010) 114105.
- [21] G. Bai, Q. Xie, J. Xu, C. Gao, Large negative piezocaloric effect: Uniaxial stress effect, *Solid State Communications* 291 (2019) 11–14.

- [22] Y. Li, J. Wang, F. Li, Intrinsic polarization switching in  $\text{BaTiO}_3$  crystal under uniaxial electromechanical loading, *Physical Review B* 94 (2016).
- [23] G. Taxil, M. Lallart, B. Ducharne, T. T. Nguyen, H. Kuwano, T. Ono, G. Sebald, Modeling of olsen cycle for pyroelectric energy harvesting and assessment of abnormal electrocaloric effect in ferroelectric single crystals, *Journal of Applied Physics* 132 (2022) 144101.
- [24] A. N. Smith, B. M. Hanrahan, Cascaded pyroelectric conversion: Optimizing the ferroelectric phase transition and electrical losses, *Journal of Applied Physics* 128 (2020) 024103.
- [25] A. Devonshire, Xcvi. theory of barium titanate, *The London, Edinburgh, and Dublin Philosophical Magazine and Journal of Science* 40 (1949) 1040–1063.
- [26] W. Cao, Constructing landau-ginzburg-devonshire type models for ferroelectric systems based on symmetry, *Ferroelectrics* 375 (2008) 28–39.
- [27] J.-Y. Li, C. H. Lei, L.-J. Li, Y.-C. Shu, Y. Liu, Unconventional phase field simulations of transforming materials with evolving microstructures, *Acta Mechanica Sinica* 28 (2012).
- [28] D. Vanderbilt, M. H. Cohen, Monoclinic and triclinic phases in higher-order devonshire theory, *Phys. Rev. B* 63 (2001) 094108.
- [29] J. H. Qiu, J. N. Ding, N. Y. Yuan, X. Q. Wang, Phase diagram of  $(1-x)\text{PbMg}_{1/3}\text{Nb}_{2/3}\text{O}_3 - x\text{PbTiO}_3$  single crystals, *Journal of Applied Physics* 117 (2015) 074101.
- [30] T. E. Hooper, A. J. Bell, Landau–devonshire derived phase diagram of the  $\text{bifeo}_3\text{-pbtio}_3$  solid solution, *Journal of Applied Physics* 127 (2020) 104102.
- [31] K. Abe, O. Furukawa, H. Imagawa, Calculations concerning the phase diagram, dielectric constant and lattice parameters for the  $\text{Pb}(\text{Zn}_{1/3}\text{Nb}_{2/3})\text{O}_3 - \text{PbTiO}_3$  solid solution, *Ferroelectrics* 87 (1988) 55–64.
- [32] P. Chandra, P. B. Littlewood, *A Landau Primer for Ferroelectrics*, Springer Berlin Heidelberg, 2007, p. 69.

- [33] T. Yoshihito, Development of large diameter piezo-single crystal pmn-pt of high energy transfer efficiency, JFE Technical Report (2005).
- [34] M. Davis, D. Damjanovic, N. Setter, Temperature dependence of the direct piezoelectric effect in relaxor-ferroelectric single crystals: Intrinsic and extrinsic contributions, *Journal of Applied Physics* 100 (2006) 084103.
- [35] S.-E. Park, T. R. Shrout, Ultrahigh strain and piezoelectric behavior in relaxor based ferroelectric single crystals, *Journal of Applied Physics* 82 (1997) 1804–1811.
- [36] A. Xue, C. Fang, C. Wang, Z. Wu, Y. Jia, Y. Liu, H. Luo, Uniaxial stress-induced ferroelectric depolarization in  $\langle 001 \rangle$ -oriented  $0.72\text{Pb}(\text{Mg}_{1/3}\text{Nb}_{2/3})\text{O}_3 - 0.28\text{PbTiO}_3$  single crystal, *Journal of Alloys and Compounds* 647 (2015) 14–17.
- [37] K. G. Webber, R. Zuo, C. S. Lynch, Ceramic and single-crystal  $(1-x)\text{pmn-xpt}$  constitutive behavior under combined stress and electric field loading, *Acta Materialia* 56 (2008) 1219–1227.
- [38] L. Yang, H. Huang, Z. Xi, L. Zheng, S. Xu, G. Tian, Y. Zhai, F. Guo, L. Kong, Y. Wang, W. Lü, L. Yuan, M. Zhao, H. Zheng, G. Liu, Simultaneously achieving giant piezoelectricity and record coercive field enhancement in relaxor-based ferroelectric crystals, *Nature Communications* 13 (2022).
- [39] E. A. McLaughlin, T. Liu, C. S. Lynch, Relaxor ferroelectric pmn-32pt crystals under stress and electric field loading: I-32 mode measurements, *Acta Materialia* 52 (2004) 3849–3857.
- [40] E. A. McLaughlin, T. Liu, C. S. Lynch, Relaxor ferroelectric pmn-32pt crystals under stress, electric field and temperature loading: Ii-33-mode measurements, *Acta Materialia* 53 (2005) 4001–4008.
- [41] J. Li, R. Yin, X. Su, H.-H. Wu, J. Li, S. Qin, S. Sun, J. Chen, Y. Su, L. Qiao, D. Guo, Y. Bai, Complex phase transitions and associated electrocaloric effects in different oriented pmn-30pt single crystals under multi-fields of electric field and temperature, *Acta Materialia* 182 (2020) 250–256.

- [42] I.-H. Kim, I.-H. Kim, S.-G. Im, K.-O. Jang, A phenomenological study on temperature-concentration-electric field phase diagram of relaxor ferroelectrics pmn-pt single crystals, *Physica B: Condensed Matter* 639 (2022) 413961.
- [43] M. Davis, D. Damjanovic, N. Setter, Electric-field-, temperature-, and stress-induced phase transitions in relaxor ferroelectric single crystals, *Phys. Rev. B* 73 (2006) 014115.
- [44] X. Zhao, J. Y. Dai, J. Wang, H. L. W. Chan, C. L. Choy, X. M. Wan, H. S. Luo, Relaxor ferroelectric characteristics and temperature-dependent domain structure in a (110)-cut  $(\text{PbMg}_{1/3}\text{Nb}_{2/3}\text{O}_3) - 0.75(\text{PbTiO}_3)_{0.25}$  single crystal, *Phys. Rev. B* 72 (2005) 064114.
- [45] J. Peräntie, H. N. Taylor, J. Hagberg, H. Jantunen, Z.-G. Ye, Electrocaloric properties in relaxor ferroelectric  $(1-x)\text{Pb}(\text{Mg}_{1/3}\text{Nb}_{2/3})\text{O}_3 - x\text{PbTiO}_3$  system, *Journal of Applied Physics* 114 (2013) 174105.
- [46] S. Patel, A. Chauhan, R. Vaish, Analysis of high-field energy harvesting using ferroelectric materials, *Energy Technology* 2 (2014) 480–485.
- [47] C. Chen, Y. Wang, J. Li, C. Wu, G. Yang, Piezoelectric, ferroelectric and pyroelectric properties of  $(1-x)\text{Pb}(\text{Mg}_{1/3}\text{Nb}_{2/3})\text{O}_3 - x\text{PbTiO}_3$  ceramics, *Journal of Advanced Dielectrics* 12 (2022) 2250002.
- [48] H. Li, H. Tian, D. Gong, Q. Meng, Z. Zhou, High dielectric tunability of  $\text{KTa}_{0.60}\text{Nb}_{0.40}\text{O}_3$  single crystal, *Journal of Applied Physics* 114 (2013) 054103.
- [49] F. Li, S. Zhang, Z. Xu, L.-Q. Chen, The contributions of polar nanoregions to the dielectric and piezoelectric responses in domain-engineered relaxor-pbtio3 crystals, *Advanced Functional Materials* 27 (2017) 1700310.